



Cite this: DOI: 10.1039/c8cc06586a

Received 13th August 2018,  
 Accepted 20th December 2018

DOI: 10.1039/c8cc06586a

rsc.li/chemcomm

## A safe and efficacious Pt(II) anticancer prodrug: design, synthesis, *in vitro* efficacy, the role of carrier ligands and *in vivo* tumour growth inhibition†

Pradip Kumar Dutta,‡<sup>a</sup> Rupali Sharma,‡<sup>a</sup> Smita Kumari,‡<sup>a</sup> Ravindra Dhar Dubey,<sup>a</sup> Sujit Sarkar,<sup>a</sup> Justin Paulraj,<sup>a</sup> Gonela Vijaykumar,<sup>b</sup> Manoj Pandey,<sup>a</sup> L. Sravanti,<sup>§c</sup> Mallik Samarla,<sup>a</sup> Hari Sankar Das,<sup>b</sup> Yashpal,<sup>a</sup> Heeralal B.,<sup>a</sup> Ravinder Goyal,<sup>a</sup> Nimish Gupta,<sup>ib ac</sup> Swadhin K. Mandal,<sup>ib b</sup> Aniruddha Sengupta\*<sup>ac</sup> and Arindam Sarkar<sup>ib \*ac</sup>

**Diaminocyclohexane-Pt(II)-phenalenyl complexes (1 and 2) showed an appropriate balance between efficacy and toxicity. Compound 2 showed nearly two-fold higher tumour growth inhibition than oxaliplatin in a murine NSCLC tumour model, when a combined drug development approach was used. The fluorescent properties of phenalene were utilized to understand the mechanistic details of the drug.**

Platinum-based drugs play an important role in cancer chemotherapy.<sup>1</sup> Despite their prevalence in cancer treatment regimens, inherent adverse effects and limitations of platinum compounds continue to plague the field.<sup>2</sup> Numerous novel platinum and other metal complexes have been designed and synthesized to develop new antitumour drugs in the past decades, with cisplatin, carboplatin and oxaliplatin representing the 1st, 2nd and 3rd generation of platinum based anticancer drugs respectively.<sup>3</sup> Despite its better tolerability compared to cisplatin, oxaliplatin is also associated with side effects such as neurotoxicity, hematologic toxicities, neutropenia, nausea, and vomiting that limit its doses.<sup>4,5</sup> Oxaliplatin and cisplatin have a similar rate of aquation which is faster than that of carboplatin,<sup>6</sup> with both drugs undergoing extensive nonenzymatic biotransformation *in vivo*, leading to non-specific toxicity.<sup>7</sup> Nucleophiles, such as endogenous proteins and small molecules containing thiol groups, displace the

oxalate group, in oxaliplatin, leading to 75–85% non-specific binding to plasma and cytosolic proteins; deactivating the drug before it reaches its target.<sup>1</sup> A subtle and appropriate balance between aquation (efficacy) and deactivation (toxicity) should solve this problem. Although numerous complexes have been prepared and tested thus far,<sup>8,9</sup> only a few additional compounds are approved for regional use in Asia.<sup>7</sup> Thus, a properly tuned Pt coordination displaying increased antitumour activity and reduced cross-resistance and toxicity is still being sought.

Phenalene is a natural product<sup>10</sup> and can be easily substituted by heteroatoms,<sup>11</sup> which can be coordinated to platinum. Phenalene based metallodrugs with an oxaliplatin backbone have not been studied till date although the application of phenalenyl (PLY) in materials science is now well-documented.<sup>12</sup> Significance of heteroatom substituted platinum phenalene compounds could be as follows: (1) easily tunable heteroatoms, containing a lone pair of electrons, could facilitate and regulate the aquation procedure in the acidic environment of tumour tissues where the heteroatoms can be protonated and the carrier ligand(phenalene) be released from the prodrug; (2) a six membered chelate of PLY to Pt could stabilize the coordination; (3) PLY can impart additional hydrophobicity which could be helpful for liposomal formulation and subsequent cellular uptake; and (4) inherent emissive characteristics of phenalene, due to intramolecular charge transfer (ICT),<sup>12c</sup> can give insight into the mechanistic details of cytotoxicity. Additionally, 1,2-diaminocyclohexane (DACH) substitution to the other two coordination sites could potentially prevent the cross resistance of new drug molecules (Scheme S1, ESI†).<sup>13</sup>

In recent years, different strategies have been embraced to incorporate platinum compounds into nanodelivery or targeted designs.<sup>14</sup> Some of these designs utilize the enhanced permeability and retention (EPR) effect, which results in preferential loading of the anticancer drugs into cancer tissues, owing to their leaky vasculature. Thus, the liposomal formulation of a carefully designed prodrug could be an effective approach to

<sup>a</sup> Invictus Oncology Pvt. Ltd., 465 Patparganj Industrial Area, Delhi 110092, India.  
 E-mail: asarkar@indiainnovationcenter.org, asengupta@indiainnovationcenter.org

<sup>b</sup> Department of Chemical Sciences, Indian Institute of Science Education and Research-Kolkata, Mohanpur – 741252, India

<sup>c</sup> India Innovation Research Center, 465 Patparganj Industrial Area, Delhi 110092, India

† Electronic supplementary information (ESI) available. Experimental procedures, characterization data, TEM images, TUNEL assay, DLS data, emission plots of ligands and complexes, and crystal data table. CCDC 1849788 and 1849789. For ESI and crystallographic data in CIF or other electronic format see DOI: 10.1039/c8cc06586a  
 ‡ These authors contributed equally.

§ All authors (except L. Sravanti and Hari Sankar Das) are either employees/ collaborators with Invictus Oncology Pvt. Ltd and/or hold equity of IOPL.

overcome some of the above-mentioned toxicity issues associated with platinum anti-cancer therapeutics.

In the current work, three different approaches of anticancer drug development have been combined: unique molecular designing, novel drug delivery systems and understanding drug-function using inherent fluorescent properties of PLY. Here we illustrate the kinetic inertness of platinum to PLY coordination in the presence of deactivating thiols, as well as demonstrated the release of a carrier ligand in cancer cells. Fluorescent “on-off” properties of the carrier ligand and its complexed forms, respectively, have been utilized to trace the released carrier ligand inside the cancer cells. Entrapment of small molecules into liposomal nanoparticles resulted in higher cellular uptake and improved *in vitro* efficacy in comparison to oxaliplatin. *In vivo* results indicate that tumour growth inhibition of the novel compound in a murine lung cancer model was significantly better than oxaliplatin.

Compounds **1** and **2** were synthesized by refluxing the corresponding phenalenone ligands **1a** and **2a**,<sup>11</sup> respectively, with aquated DACH platinum compounds (Scheme S1, ESI<sup>†</sup>) in an ethanol–water mixture and purified by recrystallization. The molecular structures of these compounds were confirmed by elemental analysis, single crystal X-ray crystallography and NMR spectroscopy. In the <sup>1</sup>H NMR spectrum, the absence of any OH or NH signal around the 11 to 13 ppm region supported the fact that anionic form of the ligand was bound to Pt. <sup>1</sup>H NMR signals for compound **1** established the fact that the PLY moiety was symmetrically coordinated to platinum. <sup>195</sup>Pt NMR signals at ~–1500 and –1800 ppm for compounds **1** and **2** indicated O,O and N,O coordination, respectively, to platinum.<sup>15</sup> In order to understand the change in emission properties due to complexation, comparative analyses of the emission spectra were performed for the ligand and corresponding metal complexes (**1** and **2**). We establish that **1** and **2** were not emissive in solution at room temperature whereas the uncomplexed forms (**1a**, **2a**) were highly emissive [ $\lambda_{(em)}$  440–475 (**1a**) and 480–520 nm (**2a**)] (Fig. S8, ESI<sup>†</sup>).

Crystals of compounds **1** and **2**, suitable for X-ray investigation, were obtained from methanol/toluene and methanol/diethylether solvent mixtures, respectively. Single crystal X-ray structures are shown in Fig. 1. Both complexes adopted roughly a square planar coordination geometry around the platinum center (as suggested from the bond angle data shown in Table S2, ESI<sup>†</sup>). The Pt–O bond lengths were around 197 pm, which is 3 pm less than the Pt–O bond length (200 pm) found in structurally related clinically approved drugs, such as oxaliplatin.<sup>16</sup> Shorter Pt–O bonds justified the stability of the prodrug.

Activation energy barriers for the 1st and 2nd aquation steps of the three proposed compounds (**1**, **2** and **3**, Scheme S1, ESI<sup>†</sup>) have been computationally evaluated for better understanding the aquation procedure and evaluation of *in vitro* efficacy.<sup>6</sup> The results depicted in Table S3 (ESI<sup>†</sup>) show that compounds **1** and **2** did not significantly differ in terms of their activation energy barrier of aquation, but compound **3** had higher energies with respect to **1** and **2** for 1st and 2nd aquation under acidic conditions. In the 1st aquation, where protonation has been

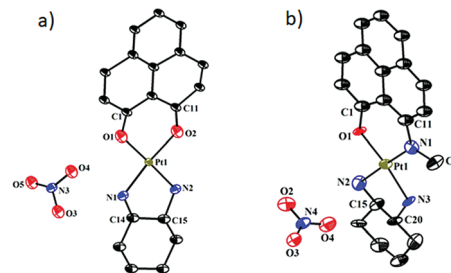
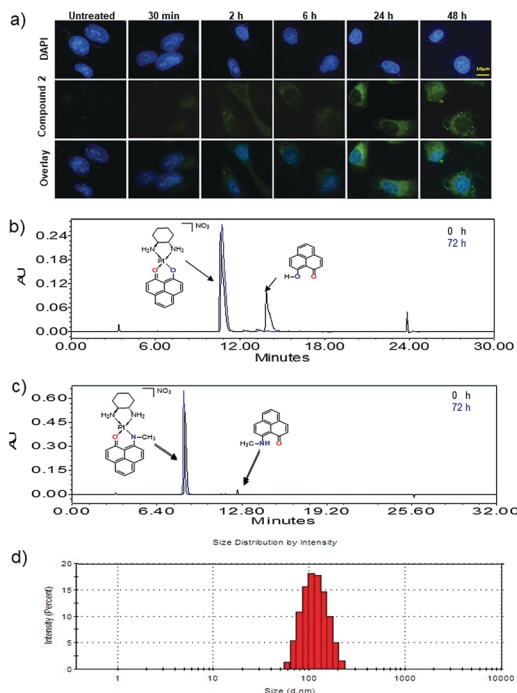


Fig. 1 Molecular structures of (a) (OO)PtPLY (**1**) and (b) (NO)PtPLY (**2**) (hydrogen atoms are not shown for the sake of clarity).

considered, a significant reduction in the activation energy barrier has been observed for **1** and **2**, indicating that the acidic tumour microenvironment would facilitate the aquation process of these two compounds.

In order to understand whether the carrier ligand was released in the cancer cell, we treated A549 cells with 5  $\mu$ M of compound **2** and visualized the cells using an epifluorescence microscope to determine the release of PLY at designated time points. Representative images clearly indicated the release of carrier ligand in a time dependent manner (Fig. 2a). Different staining patterns and intensities, obtained for uncomplexed PLY treated A549 cells, indicate that **2** is dissociated inside the cells (Fig. S9, ESI<sup>†</sup>). Using “on-off” switching to trace the ligand release was not shown in previously reported fluorescent Pt-drugs.<sup>17</sup> It has already been established that the interaction of intra and extracellular proteins or small molecules containing sulfhydryl groups inactivates platinum drugs. Thiols bind with platinum, resulting in a reduction of active platinum available for DNA binding.<sup>18</sup> The reactivity of thiols towards **1** and **2** was examined using glutathione and results in Fig. 2b and c indicate the kinetic inertness of Pt to phenalenyl coordination in the presence of glutathione ( $t_{1/2} > 72$  h). Fast degradation ( $t_{1/2} < 2$  h) of oxaliplatin or carboplatin in the presence of glutathione has already been reported<sup>19</sup> and our results indicate the release of a ligand upon reaction of **2** with 5'-GMP (Fig. S10, ESI<sup>†</sup>). Combining this result with epifluorescence images, we establish that the compound successfully internalizes in cancer cells, following which the carrier ligand releases active platinum for interaction with DNA, thus generating the necessary balance between stability and efficacy of compound **2**. We postulate that this could be a putative mechanism of action, however, other mechanisms cannot be ruled out.

Owing to low solubility of the compound in aqueous medium, a liposomal formulation was developed for *in vivo* administration of the compounds. Significant enhancement of drug solubility was observed, enabling administration of the drug in required dosage (see the ESI<sup>†</sup>). The formulation of **2** was characterized by HRTEM, (Fig. S12a, ESI<sup>†</sup>) which revealed the formation of predominant liposomal structures, less than 150 nm in diameter. Dynamic light scattering (DLS) further confirmed the homogeneous size distribution of the liposomal particles with a mean hydrodynamic diameter of  $117.6 \pm 2$  nm for **1** and  $121 \pm 9$  nm for **2** (Fig. 2d and Tables S4 and S5, ESI<sup>†</sup>), which would ensure that the drug is compartmentalized away



**Fig. 2** (a) Cellular internalization of a liposomal formulation of compound **2** in A549 cells and time dependent release of PLY. Scale bar represents 10  $\mu\text{m}$ ; (b) reactivity of **1** with glutathione in PBS shows that 88% compound remains unreacted after 72 h; (c) reactivity of **2** with glutathione in PBS shows that 89% compound remains unreacted after 72 h; (d) DLS histogram of formulated **2** shows uniform size distribution.

from healthy tissues and delivered preferentially to the tumours by EPR effect.<sup>14</sup>

Low PDI ( $<0.2$ ) indicated narrow particle size distribution and stability of formulations. *In vitro* release-kinetics data exhibited a pH-dependent sustained release of **2** (Fig. S12b, ESI<sup>†</sup>) with minimal release in PBS at physiological pH, ensuring higher availability of the drug in an acidic environment of cancer cells. Liposomal formulations of compounds **1** and **2** when evaluated for cellular cytotoxicity across human cancer lines, responsive to standard platinum therapy, showed significantly improved efficacy for **2** (Table S6, ESI<sup>†</sup>) compared to clinically approved platinum drugs oxaliplatin and carboplatin. Liposomal formulations enhance efficacy of the synthesized compounds, possibly through preferential delivery and higher accumulation in cells, hence we examined the cellular accumulation of liposomal formulations of **1** and **2** in comparison to oxaliplatin and carboplatin in A549 cells. Data reveal significantly higher uptake for the formulated compounds in comparison to the clinically approved drugs (Fig. 3a). The increased cellular accumulation of **1** and **2**, in comparison to oxaliplatin and carboplatin is consistent with the premise that hydrophobic rather than hydrophilic platinum compounds penetrate the cytoplasmic membrane more easily ( $\log P$  values are shown in Table S7, ESI<sup>†</sup>). Higher intracellular uptake and cytotoxicity of **2** can be explained by more drug loading (3 mmol of **2** vs. 2 mmol of **1**) in the liposomes. The hydrophobic nature of the compound assists in liposome formation, which in turn enhances the uptake.

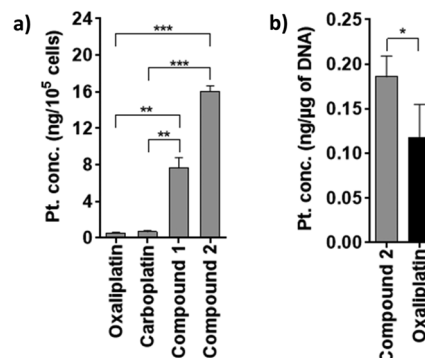


**Fig. 3** (a) Cellular uptake of compounds **1** and **2**, oxaliplatin and carboplatin in A549 cells, measured by AAS and represented as ng Pt/ $10^5$  cells. (b) The DNA–Pt adduct formation following 24 h incubation with Pt-equivalent doses of oxaliplatin or compound **2** in A549 cells, measured by AAS and represented as ng Pt/ $\mu\text{g}$  of DNA. Values are mean  $\pm$  SD (\*,  $p \leq 0.05$ ; \*\*,  $p \leq 0.005$ ; \*\*\*,  $p \leq 0.0005$ ).

Hence, for subsequent studies, a liposomal formulation of **2** was selected. Increased intracellular uptake of **2** may result in an elevated amount reaching the DNA. We evaluated the interaction of compound **2** and DNA through DNA platination following exposure of A549 cells to liposomal **2** or oxaliplatin for 24 h. Fig. 3(b) indicates higher interaction of **2** with DNA, in comparison to oxaliplatin at Pt-equivalent concentrations of compounds. Significantly high DNA-platination of compound **2** is not observed probably due to a slow reaction rate with DNA as suggested by the 5'-GMP reaction. The interaction of compound **2** with genomic-DNA was evaluated *in vitro*, and the results indicated that interaction with **2** retarded the migration of genomic-DNA on an agarose gel, through the formation of a high molecular weight complex (Fig. S13, ESI<sup>†</sup>).

Hence, these data show that in contrast to the clinically approved 2nd and 3rd generation platinum drugs, designing compounds such as **1** and **2** may be a promising approach, as their higher cellular uptake and enhanced DNA interaction would improve the therapeutic index of platinum anticancer agents.

Assessment of apoptosis is an important parameter for evaluating the response to therapy, as platinum drugs induce DNA adduct formation, leading to apoptosis, which is associated with the cytotoxicity of these drugs.<sup>1</sup> We evaluated compound mediated apoptosis for oxaliplatin and **2** at equivalent Pt-concentrations in A549 cells. TUNEL results indicated that the treatment with compound **2** leads to higher apoptosis ( $\sim 60\%$ ) in A549 cells in comparison to oxaliplatin ( $\sim 20\%$ ) under identical experimental conditions (Fig. S14, ESI<sup>†</sup>).

The antitumour activity of compound **2** was compared to oxaliplatin in a murine NSCLC tumour model (LLC tumour). Chemotherapy remains the standard first-line therapy for the majority of NSCLC patients with an advanced stage of the disease, of which platins are considered the most efficacious option.<sup>20</sup> The goal for new platinum agents to be tested in NSCLC is to maintain or improve the efficacy and/or reduce toxicity. Oxaliplatin based first line therapy for NSCLC tumour models has been undergoing clinical trials and showing similar results to that of other clinically approved platinum therapeutics.<sup>21</sup>

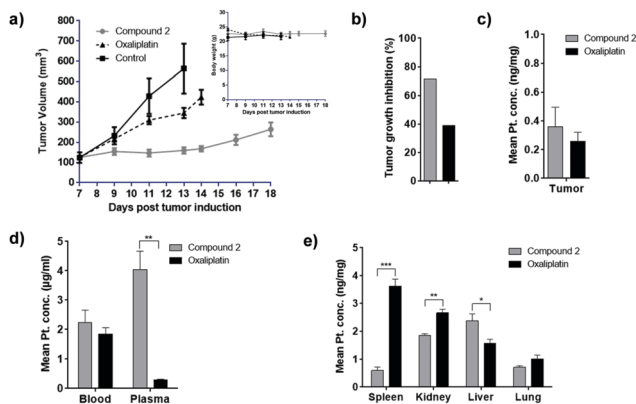


**Fig. 4** (a) Antitumour activity of compound **2** and oxaliplatin was evaluated in syngeneic LLC tumour model. The mice were implanted with  $1 \times 10^6$  LLC cells and grouped as untreated (control), oxaliplatin and compound **2** treated. The tumour volume and body weight of the treated animals were recorded. (b) Tumour growth inhibition measurement for mice treated with compound **2** and oxaliplatin. The biodistribution of the tested compounds was recorded in (c) tumour, (d) plasma and blood, and (e) other tissues (\*,  $p \leq 0.05$ ; \*\*,  $p \leq 0.005$ ; \*\*\*,  $p \leq 0.0005$ ).

Treatment with compound **2** led to a substantial reduction in tumour volume (Fig. 4a), with a tumour growth inhibition (TGI) of  $\sim 72\%$ , in comparison to  $\sim 39\%$  observed for oxaliplatin treatment, emphasizing on the *in vivo* potency of compound **2** (Fig. 4b). We did not observe any decrease in the body weight of the mice across treatment groups for the experimental period, ruling out any systemic toxicity associated with compound **2** (Fig. 4a, inset).

Platinum accumulation in tumours was evaluated 1 week after the last compound dose and we observed a higher Pt accumulation in tumours treated with compound **2** (Fig. 4c). Biodistribution of the compounds was evaluated in C57/BL6 mice, 24 hours post single i.v. injection of  $5 \text{ mg Pt kg}^{-1}$  dose of compounds. Our findings reveal comparable Pt detection in the whole blood, but a significantly higher amount of platinum in plasma, suggesting non-binding of compound **2** to RBCs and higher availability in plasma (Fig. 4d). Tissue distribution showed a significantly lower accumulation of compound **2** in spleen in comparison to oxaliplatin (Fig. 4e). Biodistribution of **2** and oxaliplatin in tumour bearing mice is shown in Fig. S15 (ESI†).

In summary, we have successfully implemented a combined drug development approach, proposed three PLY based platinum molecules as anticancer drugs, and selected two of them for synthesis and detailed characterization, corroborating the computational outcome on activation energy barriers of aquation on the platinum center. Compounds **1** and **2** showed increased *in vitro* stability in the presence of thiols in comparison to oxaliplatin but released the carrier ligand and effector molecule inside cancer cells. Enhanced hydrophobicity resulting from PLY substitution enables liposomal entrapment of the compounds, ensuring higher cellular uptake and superior cellular cytotoxicity across human cancer lines. An appropriate balance between efficacy and toxicity is supported by *in vivo* studies in the syngeneic murine NSCLC tumour model. Furthermore, treatment with compound **2** did not lead to thrombocytopenia

or splenomegaly (toxicities commonly associated with oxaliplatin), which could potentially enable higher dosage administration, thereby improving the clinical outcome.

This work was financially supported by the Science and Engineering Research Board (SERB) (Project EMR/2016/000357). The authors gratefully acknowledge the use of the services and analytical facility of IISER Kolkata funded by IISER-IOP technical grant.

## Conflicts of interest

There are no conflicts to declare.

## Notes and references

- 1 T. C. Johnstone, K. Suntharalingam and S. J. Lippard, *Chem. Rev.*, 2016, **116**, 3436–3486.
- 2 C. A. Rabik and M. E. Dolan, *Cancer Treat. Rev.*, 2007, **33**, 9–23.
- 3 (a) N. J. Farrer, L. Salassa and P. J. Sadler, *Dalton Trans.*, 2009, 10690–10701; (b) P. C. A. Bruijninx and P. J. Sadler, *Curr. Opin. Chem. Biol.*, 2008, **12**, 197–206; (c) C. G. Hartinger, N. M. Nolte and P. J. Dyson, *Organometallics*, 2012, **31**, 5677–5685; (d) M. Galanski, M. A. Jakupec and B. K. Keppler, *Curr. Med. Chem.*, 2005, **12**, 2075–2094.
- 4 T. Boulikas, A. Pantos, E. Bellis and P. Christofis, *Cancer Ther.*, 2007, **5**, 537–583.
- 5 L. Kelland, *Nat. Rev. Cancer*, 2007, **7**, 573–584.
- 6 M. F. A. Lucas, M. Pavelka, M. E. Alberto and N. Russo, *J. Phys. Chem. B*, 2009, **113**, 831–838.
- 7 M. A. Graham, G. F. Lockwood, D. Greenslade, S. Brienza, M. Bayssas and E. Gamelin, *Clin. Cancer Res.*, 2000, **6**, 1205–1218.
- 8 E. Wong and C. M. Giandomenico, *Chem. Rev.*, 1999, **99**, 2451.
- 9 K. S. Lovejoy and S. J. Lippard, *Dalton Trans.*, 2009, 10651–10659.
- 10 F. Carnovale, T. H. Gan, J. B. Peel and K. D. Franz, *J. Chem. Soc., Perkin Trans. 2*, 1980, 957–960.
- 11 K. D. Franz and R. L. Martin, *Tetrahedron*, 1978, **34**, 2147.
- 12 (a) K. V. Raman, A. M. Kamerbeek, A. Mukherjee, N. Adiresei, T. K. Sen, P. Lazi, V. Caciuc, R. Michel, D. Stalke, S. K. Mandal, S. Blügel, M. Münzenberg and J. S. Moodera, *Nature*, 2013, **493**, 509–513; (b) S. K. Pal, M. E. Itkis, F. S. Tham, R. W. Reed, R. T. Oakley and R. C. Haddon, *Science*, 2005, **309**, 281–284; (c) A. Mitra, A. Pariyar, S. Bose, P. Bandyopadhyay and A. Sarkar, *Sens. Actuators, B*, 2015, **210**, 712–718.
- 13 H. G. Koch, *Rev. Physiol., Biochem. Pharmacol.*, 2003, **146**, 1–53.
- 14 (a) S. Mukhopadhyay, C. M. Barnés, A. Haskel, S. M. Short, K. R. Barnes and S. J. Lippard, *Bioconjugate Chem.*, 2008, **19**, 39–49; (b) S. Dhar, Z. Liu, J. Thomale, H. Dai and S. J. Lippard, *J. Am. Chem. Soc.*, 2008, **130**, 11467–11476; (c) S. Dhar, W. L. Daniel, D. A. Giljohann, C. A. Mirkin and S. J. Lippard, *J. Am. Chem. Soc.*, 2009, **131**, 14652–14653; (d) H. Yin, L. Liao and J. Fang, *JSM Clin. Oncol. Res.*, 2014, **2**, 1010; (e) J. S. Butler and P. J. Sadler, *Curr. Opin. Chem. Biol.*, 2013, **17**, 1–14; (f) D. Liu, C. He, A. Z. Wang and W. Lin, *Int. J. Nanomed.*, 2013, **20**, 3309–3319.
- 15 E. Gabano, E. Marengo, M. Bobba, E. Robotti, C. Cassino, M. Botta and D. Osella, *Coord. Chem. Rev.*, 2006, **250**, 2158.
- 16 M. A. Bruck and R. Bau, *Inorg. Chim. Acta*, 1984, **92**, 279–284.
- 17 (a) M. A. Miller, B. Askevold, K. S. Yang, R. H. Kohler and R. Weissleder, *ChemMedChem*, 2014, **9**, 1131–1135; (b) S. Banerjee, J. A. Kitchen, S. A. Bright, J. E. O'Brien, D. C. Williams, J. M. Kelly and T. Gunnlaugsson, *Chem. Commun.*, 2013, **49**, 8522–8524; (c) Z. Chen, S. Zhang, L. Shen, Z. Zhu and J. Zhang, *New J. Chem.*, 2015, **39**, 1592–1596.
- 18 Z. Wang, M. Wu and S. J. Gou, *Inorg. Biochem.*, 2016, **157**, 1–7.
- 19 L. Sercombe, T. Veerati, F. Moheimani, S. Y. Wu, A. K. Sood and S. Hua, *Front. Pharmacol.*, 2015, **6**, 286.
- 20 (a) A. Rossi and M. D. Maio, *Expert Rev. Anticancer Ther.*, 2016, **16**, 653–660; (b) L. Bonanno, A. Favaretto and R. Rosell, *Anticancer Res.*, 2014, **34**, 493–501.
- 21 (a) L. E. Ræz, S. Kobina and E. S. Santos, *Clin. Lung Cancer*, 2010, **1**, 18–24; (b) <https://clinicaltrials.gov/ct2/home>.